ARTICLE IN PRESS

Computer Physics Communications ▮ (▮▮▮▮) ▮▮▮–▮▮▮

Contents lists available at ScienceDirect

Computer Physics Communications

journal homepage: www.elsevier.com/locate/cpc

Mode Gaussian beam tracing

M.Yu. Trofimov *, A.D. Zakharenko, S.B. Kozitskiy

Il'ichev Pacific Oceanological Institute, 43 Baltiyskay str., Vladivostok, 690041, Russia

ARTICLE INFO

Article history:
Received 20 November 2015
Received in revised form
11 May 2016
Accepted 6 June 2016
Available online xxxx

Keywords:
Parabolic equation method
Multiple-scale method
Normal mode
Gaussian beam

ABSTRACT

A mode parabolic equation in the ray centered coordinates for 3D underwater sound propagation is developed. The Gaussian beam tracing in this case is constructed. The test calculations are carried out for the ASA wedge benchmark and proved an excellent agreement with the source images method in the case of cross-slope propagation. But in the cases of wave propagation at some angles to the cross-slope direction an account of mode interaction becomes necessary.

1. Introduction

The problem of sound propagation by the method of summation of Gaussian beams was considered in [1–6]. In these papers the absence of singularities appropriate to the ray methods (such as caustics) was proven and also the tuning of the method was performed. In the present paper we consider a method of mode Gaussian beams, which enables to treat 3D problems. In this study a method of Gaussian beams is amalgamated with the normal mode theory. More precisely, the equations for the mode amplitudes are reduced to the parabolic equations that are subsequently solved along the horizontal rays. This approach may be considered as the direct generalization of vertical modes + horizontal rays method of Burridge and Weinberg [7], yet it also incorporates some features of the mode parabolic equations theory. In the frame of the proposed method we do not consider the mode interaction.

The problem of sound propagation in a three-dimensional wedge is solved by the developed method. It appears that in the case of the cross-slope propagation the method gives very accurate results despite the absence of the mode interaction in our model. Moreover it is necessary to consider only the exited modes which present explicitly in the final solution. On the other hand, in the parabolic equation [8,9] we should consider the large number of modes with their interactions. Thus, many effects previously described in the terms of the mode interaction can be explained in the terms of the horizontal refraction.

In the case when the angle of the track of sound propagation to the across slope direction gradually increases it becomes necessary to account for the mode interaction. It is shown, that at the angle of 18° the mode interaction becomes significant and further increases. The mode interaction is therefore essential for the more general models of sound propagation.

The paper is organized as follows. After formulation of the problem in Section 2, we consider an adiabatic mode Helmholtz equation. Then, by using Babich method, we obtain a mode parabolic equation in the ray centered coordinates from the derived Helmholtz equation. In Section 4 we discuss certain details related to mode Gaussian beams propagation. In Section 5 the method of mode Gaussian beams is used for the numerical solution of the ASA wedge benchmark problem in the case of cross-slope wave propagation and in the cases of wave propagation at various angles to the cross-slope direction. The results are compared with the solutions obtained by the method of image sources and by adiabatic mode parabolic equations. The paper ends with a brief conclusion.

2. Basic equations and boundary conditions

We consider the propagation of time-harmonic sound in a three-dimensional waveguide

$$\Omega = \{(x, y, z) | 0 \le x \le \infty, -\infty \le y \le \infty, -H \le z \le 0\}$$

(the z-axis is directed upward), described by the acoustic Helmholtz equation

$$(\gamma P_x)_x + \left(\gamma P_y\right)_y + (\gamma P_z)_z + \gamma \kappa^2 P = 0, \tag{1}$$

where $\gamma = 1/\rho$, $\rho = \rho(x, y, z)$ is the density, κ is the wave-number. We assume the appropriate radiation conditions at

* Corresponding author.
E-mail address: trofimov@poi.dvo.ru (M.Yu. Trofimov).

http://dx.doi.org/10.1016/j.cpc.2016.06.002
0010-4655/

infinity in the x, y plane, the pressure-release boundary condition $P = 0$ at $z = 0$ and the rigid boundary condition $\partial P/\partial z = 0$ at $z = -H$. The parameters of the medium can be discontinuous at the nonintersecting smooth interfaces $z = h_1(x, y), \ldots, h_m(x, y)$, where the usual interface conditions

$$P_+ = P_-,$$
$$\gamma_+ \left(\frac{\partial P}{\partial z} - h_x \frac{\partial P}{\partial x} - h_y \frac{\partial P}{\partial y} \right)_+ = \gamma_- \left(\frac{\partial P}{\partial z} - h_x \frac{\partial P}{\partial x} - h_y \frac{\partial P}{\partial y} \right)_- , \quad (2)$$

are imposed. Hereafter the denotations $f(z_0, x, y)_+ = \lim_{z \downarrow z_0} f(z, x, y)$ and $f(z_0, x, y)_- = \lim_{z \uparrow z_0} f(z, x, y)$ are used. As will be shown below, it is sufficient to consider the case of $m = 1$, so we set $m = 1$ and denote h_1 by h.

We introduce a small parameter ϵ (the ratio of the typical wavelength to the typical size of medium inhomogeneities), the slow variables $X = \epsilon x$ and $Y = \epsilon y$ and the fast variables $\eta = (1/\epsilon)\Theta(X, Y)$ and $\xi = (1/\sqrt{\epsilon})\Psi(X, Y)$ and postulate the following expansions for the acoustic pressure P and the parameters κ^2, γ and h:

$$\begin{aligned} P &= P_0(X, Y, z, \eta, \xi) + \sqrt{\epsilon} P_{1/2}(X, Y, z, \eta, \xi) + \cdots, \\ \kappa^2 &= n_0^2(X, Y, z) + \epsilon \nu(X, Y, z, \xi), \\ \gamma &= \gamma_0(X, Y, z) + \epsilon \gamma_1(X, Y, z, \xi), \\ h &= h_0(X, Y) + \epsilon h_1(X, Y, \xi). \end{aligned} \quad (3)$$

To model the attenuation effects, we allow ν to be complex. More precisely, we put $\mathrm{Im}\nu = 2\mu\beta n_0^2$, where $\mu = (40\pi \log_{10} \mathrm{e})^{-1}$ and β is the attenuation in decibels per wavelength.

Following the generalized multiple-scale method [10], we replace the derivatives in Eq. (1) according to the rules

$$\frac{\partial}{\partial x} \to \epsilon \left(\frac{\partial}{\partial X} + \frac{1}{\sqrt{\epsilon}} \Psi_X \frac{\partial}{\partial \xi} + \frac{1}{\epsilon} \Theta_X \frac{\partial}{\partial \eta} \right),$$
$$\frac{\partial}{\partial y} \to \epsilon \left(\frac{\partial}{\partial Y} + \frac{1}{\sqrt{\epsilon}} \Psi_Y \frac{\partial}{\partial \xi} + \frac{1}{\epsilon} \Theta_Y \frac{\partial}{\partial \eta} \right).$$

Given the postulated expansions, the equation under consideration becomes

$$\begin{aligned} &\epsilon^2 \left(\frac{\partial}{\partial X} + \frac{1}{\sqrt{\epsilon}} \Psi_X \frac{\partial}{\partial \xi} + \frac{1}{\epsilon} \Theta_X \frac{\partial}{\partial \eta} \right) \Bigg((\gamma_0 + \epsilon\gamma_1) \\ &\cdot \left(\frac{\partial}{\partial X} + \frac{1}{\sqrt{\epsilon}} \Psi_X \frac{\partial}{\partial \xi} + \frac{1}{\epsilon} \Theta_X \frac{\partial}{\partial \eta} \right) \cdot (P_0 + \epsilon P_1 + \cdots,) \Bigg) \\ &+ \text{the same term with the } Y\text{-derivatives} \\ &+ ((\gamma_0 + \epsilon\gamma_1)(P_{0z} + \epsilon P_{1z} + \cdots,))_z \\ &+ (\gamma_0 + \epsilon\gamma_1)(n_0^2 + \epsilon\nu)(P_0 + \epsilon P_1 + \cdots,) = 0. \end{aligned} \quad (4)$$

We now put

$$P_0 + \epsilon P_1 + \cdots = (A_0(X, Y, z, \xi) + \epsilon A_1(X, Y, z, \xi) + \cdots) \mathrm{e}^{\mathrm{i}\eta}.$$

Using the Taylor expansion, we can formulate the interface conditions at h_0 which are equivalent to interface conditions (2) up to $O(\epsilon)$:

$$(A_0 + \epsilon h_1 A_{0z} + \epsilon A_1)_+ = (\text{the same terms})_-, \quad (5)$$
$$\begin{aligned} &((\gamma_0 + \epsilon h_1 \gamma_{0z} + \epsilon\gamma_1) \\ &\quad \times (A_{0z} + \epsilon h_1 A_{0zz} + \epsilon A_{1z} - \epsilon \mathrm{i}\Theta_X h_{0X} A_0 - \epsilon \mathrm{i}\Theta_Y h_{0Y} A_0))_+ \\ &= (\text{the same terms})_- . \end{aligned} \quad (6)$$

2.1. The problem at $O(\epsilon^0)$

At $O(\epsilon^0)$ we obtain

$$(\gamma_0 A_{0z})_z + \gamma_0 n_0^2 A_0 - \gamma_0 \left((\Theta_X)^2 + (\Theta_Y)^2 \right) A_0 = 0, \quad (7)$$

with the interface conditions $A_{0+} = A_{0-}$, $(\gamma_0 A_{0z})_+ = (\gamma_0 A_{0z})_-$ at $z = h_0$, and the boundary conditions $A_0 = 0$ at $z = 0$ and $A_{0z} = 0$ at $z = -H$. We seek a solution to problem (7) in the form

$$A_0 = B_j(X, Y, \xi)\phi(X, Y, z). \quad (8)$$

From Eq. (7) we obtain the following spectral problem for ϕ with the spectral parameter $k^2 = (\Theta_X)^2 + (\Theta_Y)^2$

$$\begin{aligned} &(\gamma_0 \phi_z)_z + \gamma_0 n_0^2 \phi - \gamma_0 k^2 \phi = 0, \\ &\phi(0) = 0, \qquad \phi_z = 0 \quad \text{at } z = -H, \\ &\phi_+ = \phi_-, \qquad (\gamma_0 \phi_z)_+ = (\gamma_0 \phi_z)_- \quad \text{at } z = h_0. \end{aligned} \quad (9)$$

This spectral problem, considering in the Hilbert space $L_{2,\gamma_0}[-H, 0]$ with the scalar product

$$(\phi, \psi) = \int_{-H}^{0} \gamma_0 \phi \psi \, dz, \quad (10)$$

has countably many solutions (k_j^2, ϕ_j), $j = 1, 2, \ldots$ where the eigenfunctions can be chosen as real functions. The eigenvalues k_j^2 are real and have $-\infty$ as a single accumulation point. The normalizing condition is

$$(\phi, \phi) = \int_{-H}^{0} \gamma_0 \phi^2 \, dz = 1. \quad (11)$$

2.2. The problem at $O(\epsilon^{1/2})$ and at $O(\epsilon^1)$

The solvability condition for the problem at $O(\epsilon^{1/2})$ is

$$\Theta_X \Psi_X + \Theta_Y \Psi_Y = 0, \quad (12)$$

from which we conclude that we can take $P_{1/2} = 0$.

2.3. The problem at $O(\epsilon^1)$

At $O(\epsilon^1)$, we obtain

$$\begin{aligned} &(\gamma_0 A_{1z})_z + \gamma_0 n_0^2 A_1 - \gamma_0 k_j^2 A_1 \\ &= -\mathrm{i}\gamma_{0X} k_j A_0 - 2\mathrm{i}\gamma_0 k_j A_{0X} - \mathrm{i}\gamma_0 k_{jX} u_0 + \gamma_1 k_j^2 A_0 - \gamma_0 (\Psi_X)^2 A_{0\xi\xi} \\ &\quad - \text{the same terms with } Y\text{-derivatives} \\ &\quad - \frac{\partial}{\partial z}(\gamma_1 A_{0z}) - n_0^2 \gamma_1 A_0 - \nu\gamma_0 A_0, \end{aligned} \quad (13)$$

with the boundary conditions $A_1 = 0$ at $z = 0$, $A_{1z} = 0$ at $z = -H$, and the interface conditions at $z = h_0(X, Y)$:

$$\begin{aligned} &A_{1+} - A_{1-} = h_1(A_{0z-} - A_{0z+}), \\ &\gamma_{0+} A_{1z+} - \gamma_{0-} A_{1z-} \\ &\quad = h_1 \left(((\gamma_0 A_{0z})_z)_- - ((\gamma_0 A_{0z})_z)_+ \right) + \gamma_{1-} A_{0z-} - \gamma_{1+} A_{0z+} \\ &\quad\quad - \mathrm{i}k_j h_{0X} A_0 (\gamma_{0-} - \gamma_{0+}) - \mathrm{i}k_j h_{0Y} A_0 (\gamma_{0-} - \gamma_{0+}). \end{aligned} \quad (14)$$

Multiplying (13) by ϕ_j and then integrating the resulting equation twice from $-H$ to 0 by parts with the use of the corresponding interface conditions (14), we obtain the solvability condition for the problem at $O(\epsilon^1)$

$$\begin{aligned} &2\mathrm{i}(\Theta_{jX} B_{jX} + \Theta_{jY} B_{jY}) + \mathrm{i}(\Theta_{jXX} + \Theta_{jYY}) B \\ &\quad + ((\Psi_X)^2 + (\Psi_Y)^2) B_{j\xi\xi} + \alpha_j B_j = 0, \end{aligned} \quad (15)$$

where $A_0 = B_j \phi_j$ and α_j is given by the following formula

$$\begin{aligned} \alpha_j = &\int_{-\infty}^{0} \gamma_0 \nu \phi_j^2 \, dz + \int_{-\infty}^{0} \gamma_1 \left(n_0^2 - k_j^2 \right) \phi_j^2 \, dz - \int_{-\infty}^{0} \gamma_1 \left(\phi_{jz} \right)^2 dz \\ &+ \Big\{ h_1 \phi_j \left[\left((\gamma_0 \phi_{jz})_z \right)_+ - \left((\gamma_0 \phi_{jz})_z \right)_- \right] \\ &- h_1 \gamma_0^2 \left(\phi_{jz} \right)^2 \left[\left(\frac{1}{\gamma_0} \right)_+ - \left(\frac{1}{\gamma_0} \right)_- \right] \Big\} \Big|_{z = h_0} . \end{aligned}$$

Please cite this article in press as: M.Yu. Trofimov, et al., Mode Gaussian beam tracing, Computer Physics Communications (2016), http://dx.doi.org/10.1016/j.cpc.2016.06.002

Using the spectral problem (9), the interface terms introduced above can be rewritten also as

$$\left\{h_1\phi_j^2\left[k_j^2\left(\gamma_{0+}-\gamma_{0-}\right)-\left(n_0^2\gamma_0\right)_+ +\left(n_0^2\gamma_0\right)_-\right]\right.$$
$$\left.-h_1\gamma_0^2\left(\phi_{jz}\right)^2\left[\left(\frac{1}{\gamma_0}\right)_+-\left(\frac{1}{\gamma_0}\right)_-\right]\right\}\Big|_{z=h_0}.$$

3. The adiabatic mode Helmholtz equation and the ray parabolic equation in ray centered coordinates

To obtain the adiabatic mode Helmholtz equation from Eq. (15), we introduce the new amplitude

$$D_j(x,y)=B_j(X,Y,\xi),$$

where $(x,y)=\frac{1}{\epsilon}(X,Y)$ are the initial (physical) coordinates. One can easily obtain the following formulas for the x-derivatives of D_j:

$$D_{jx}=B_{j\xi}\cdot\sqrt{\epsilon}\Psi_X+\epsilon B_{jX}, \tag{16}$$

$$D_{jxx}=B_{j\xi\xi}\cdot\epsilon(\Psi_X)^2+\epsilon^{3/2}(2B_{j\xi X}\Psi_X+B_{j\xi}\Psi_{XX})+\epsilon^2B_{jXX}, \tag{17}$$

and analogous formulas for the y-derivatives.

The solvability condition for the problem at $O(\epsilon^{3/2})$ is written as

$$2B_{j\xi X}\Psi_X+B_{j\xi}\Psi_{XX}+2B_{j\xi Y}\Psi_Y+B_{j\xi}\Psi_{YY}=0.$$

Substituting the obtained expressions for the derivatives into Eq. (15) we obtain after some algebra the reduced Helmholtz equation for D

$$2\mathrm{i}(\theta_xD_{jx}+\theta_xD_{jy})+\mathrm{i}(\theta_{xx}+\theta_{yy})D_j+D_{jxx}+D_{jyy}+\bar{\alpha}_jD_j=0, \tag{18}$$

where $\theta(x,y)=\frac{1}{\epsilon}\Theta(X,Y)$, $\bar{\alpha}_j=\epsilon\alpha_j$.

This equation can be transformed into the usual Helmholtz equation

$$\bar{D}_{jxx}+\bar{D}_{jyy}+k^2\bar{D}_j+\bar{\alpha}_j\bar{D}_j=0, \tag{19}$$

where $k^2=(\theta_x)^2+(\theta_y)^2$ by the substitution $\bar{D}_j=D_j\exp(\mathrm{i}\theta)$. Consider the ray equations for the Hamilton–Jacobi equation

$$(\theta_x)^2+(\theta_y)^2=\mathcal{P}^2+\mathcal{Q}^2=k^2$$

in the form

$$x_t=\frac{\mathcal{P}}{k},\qquad y_t=\frac{\mathcal{Q}}{k},\qquad \mathcal{P}_t=k_x,\qquad \mathcal{Q}_t=k_y. \tag{20}$$

We have $(x_t)^2+(y_t)^2=1$, so t is a natural parameter for the ray, and introduce $\vec{n}$ to be orthogonal to the ray (ray-centered coordinates).

To obtain the ray parabolic equation in the ray-centered coordinates, we first rewrite Eq. (19) in the slow variables $(X,Y)=(\epsilon x,\epsilon y)$ (ray scaling)

$$\epsilon^2\bar{D}_{jxx}+\epsilon^2\bar{D}_{jyy}+k^2\bar{D}_j+\epsilon\alpha_j\bar{D}_j=0. \tag{21}$$

Then, in the vicinity of a given ray, Eq. (21) can be written in the form

$$\epsilon^2\frac{1}{h}\left(\frac{1}{h}\bar{D}_{jt}\right)_t+\epsilon^2\frac{1}{h}(h\bar{D}_{jn})_n+k^2\bar{D}_j+\epsilon\alpha_j\bar{D}_j=0, \tag{22}$$

where t is a natural parameter of the ray (arc length), and n is the distance from a given point to the ray (in ray-centered coordinates) and $h=1-\frac{k_1}{k_0}n$. Hereafter we use the following notations for any given function $f=f(t,n)$: $f_0=f|_{n=0}$, $f_1=f_n|_{n=0}$ and $f_2=f_{nn}|_{n=0}$.

Substituting into Eq. (22) the Taylor expansions

$$k^2=k_0^2+2k_1k_0n+(k_1^2+k_0k_2)n^2$$
$$=k_0^2+\sqrt{\epsilon}2k_1k_0N+\epsilon(k_1^2+k_0k_2)N^2,$$
$$\frac{1}{h}=1+\frac{k_1}{k_0}n+\frac{k_1^2}{k_0^2}n^2=1+\sqrt{\epsilon}\frac{k_1}{k_0}N+\epsilon\frac{k_1^2}{k_0^2}N^2,$$
$$\frac{1}{h^2}=1+2\frac{k_1}{k_0}n+3\frac{k_1^2}{k_0^2}n^2=1+\sqrt{\epsilon}2\frac{k_1}{k_0}N+\epsilon3\frac{k_1^2}{k_0^2}N^2,$$

where $N=\frac{1}{\sqrt{\epsilon}}$ (parabolic scaling), and the WKB-ansatz $\bar{D}_j=(u_0+\epsilon u_1+\cdots)\exp((\mathrm{i}/\epsilon)\theta)$, we obtain at $O(\epsilon^0)$

$$\theta_t=\mathrm{i}k_0$$

and at $O(\epsilon^1)$ the parabolic equation in the ray-centered coordinates [11]

$$2\mathrm{i}k_0u_{0t}+\mathrm{i}k_{0t}u_0+u_{0NN}+[(k_0k_2-2k_1^2)N^2+\alpha_{j0}]u_0=0. \tag{23}$$

4. Mode Gaussian beam equation

To solve Eq. (23), we first introduce the following substitution:

$$u_0(t,N)=\frac{1}{\sqrt{k_0(t)}}\exp\left(\frac{\mathrm{i}}{2}\int_0^t\frac{\alpha_{j0}(s)}{k_0(s)}\,ds\right)U_j(t,N). \tag{24}$$

Then our equation becomes

$$2\mathrm{i}k_0U_{jt}+U_{jNN}+(k_0k_2-2k_1^2)N^2U_j=0. \tag{25}$$

Following [1], we seek a solution of this equation in the form of the Gaussian beam ansatz

$$U_j(t,N)=A(t)\exp\left(\frac{\mathrm{i}}{2}N^2\Gamma(t)\right), \tag{26}$$

where $\Gamma(t)$ is an unknown complex-valued function. Substitution of (26) into (25) gives

$$\mathrm{i}(2k_0A_t+A\Gamma)-AN^2[k_0\Gamma_t+\Gamma^2-(k_0k_2-2k_1^2)]=0.$$

We require separately

$$k_0\Gamma_t+\Gamma^2-(k_0k_2-2k_1^2)=0,\quad\text{and}\quad 2k_0A_t+A\Gamma=0. \tag{27}$$

To solve the first ordinary non-linear differential equation of the Riccati type, we introduce new complex-valued variables $q(t)$ and $p(t)$ by the formulas

$$\Gamma=\frac{k_0}{q}q_t=\frac{p}{q}.$$

Then

$$q_t=k_0^{-1}p,\qquad p_t=(k_2-2k_1k_0^{-1})q. \tag{28}$$

The solution of the second equation in (27) can be expressed in the following form

$$A(t)=\frac{\Psi}{\sqrt{q(t)}},$$

where Ψ is a complex value, which is constant along the ray, but may vary at different rays.

Finally for u_0 we have:

$$u_0(t,N)=\frac{\Psi(\varphi)}{\sqrt{k_0(t)q(t)}}\exp\left(\frac{\mathrm{i}}{2}\int_0^t\frac{\alpha_{j0}(s)}{k_0(s)}\,ds+\frac{\mathrm{i}}{2}N^2\frac{p(t)}{q(t)}\right). \tag{29}$$

Here φ is the parameter, that parameterizes the rays. For p and q we have the system of ordinary differential equations (28), which can be solved simultaneously with the ray equations (20). It is

Please cite this article in press as: M.Yu. Trofimov, et al., Mode Gaussian beam tracing, Computer Physics Communications (2016), http://dx.doi.org/10.1016/j.cpc.2016.06.002

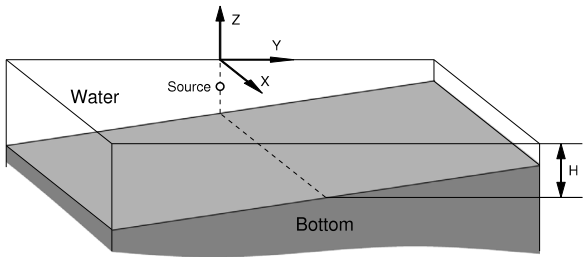

Fig. 1. The geometry for the ASA wedge benchmark. The wedge angle is ≈2.86° with a distance to the apex 4 km. The source is located at depth 100 m. The bottom depth at the place of the source $H = 200$ m.

convenient to split variables p and q onto real and imaginary parts as follows $p = p_2 - i\varepsilon p_1, q = q_2 - i\varepsilon q_1$ where ε is a sufficiently large positive real number, defining the width of the Gaussian beam. As shown in [1] and discussed in [2], the choice $\varepsilon = L_r$ ensures the minimal value of the Gaussian beam width at the receiver point in a homogeneous medium, where L_r is the arc length of the ray from the source to the receiver. Initial conditions for p and q are as follows

$$q_1(0) = 1, \qquad p_1(0) = 0, \qquad q_2(0) = 0, \qquad p_2(0) = k_0(0).$$

The acoustic field at the point M can be expressed as the integral over all rays

$$p(M) = \int_0^{2\pi} \frac{\Psi(\varphi)}{\sqrt{k_0(t)q(t)}} \exp\left[i \int_0^t \left(k_0(s) + \frac{\alpha_{j0}(s)}{2k_0(s)} \right) ds + \frac{i}{2} N^2 \frac{p(t)}{q(t)} \right] d\varphi. \tag{30}$$

Here t and N are the ray-centered coordinates of the receiver point for each ray.

One can determine the value of $\Psi(\varphi)$ by comparing the following two fields. First, the one obtained for the homogeneous medium from the formula (30) by the steepest descent method. Second, the one obtained from the fundamental solution of the Helmholtz equation for this case. So we have

$$\Psi = \frac{\phi(z_s)\phi(z_r)}{\rho(z_s)} \cdot \sqrt{ik_0(0)\varepsilon} \cdot \sqrt{1 - \frac{\alpha_{j0}(0)x}{2ik_0(0)^2\varepsilon}} \left(1 + \frac{\alpha_{j0}(0)}{2k_0(0)^2} \right)^{-1}.$$

5. Numerical experiments

We consider the case of cross-slope propagation in a standard ASA wedge benchmark problem with the wedge angle ≈2.86° (see Fig. 1). The typical bottom depth is 200 m along the track aligned along the X axis for $X = 0 \ldots 25$ km, but it can vary in some experiments from 159 to 286.5 m. The sound speed in the water is 1500 m/s. The sound speed in the fluid bottom is 1700 m/s. The bottom density is 1500 kg/m^3, the water density is 1000 kg/m^3. We assume that there is no attenuation in the water column, while in the bottom the attenuation is 0.5 dB/λ. In the all cases the point source is located at depth 100 m, and depth of receivers is 30 m. For calculation purposes we restrict the total depth to 600 m.

To illustrate the efficiency of our equation, we performed 3 series of numerical experiments. In the first series of experiments (see Figs. 2–4), we investigate the cross-slope sound propagation for the standard ASA wedge benchmark up to distance 25 km. In Fig. 2, we present comparisons between the solution of our equation with only 3 propagating modes and the image sources solution [12]. One can see that the curves are quite close, and the root mean square difference between curves is about 1.4 dB. To improve the accuracy of the method on the first 1.5 km we can

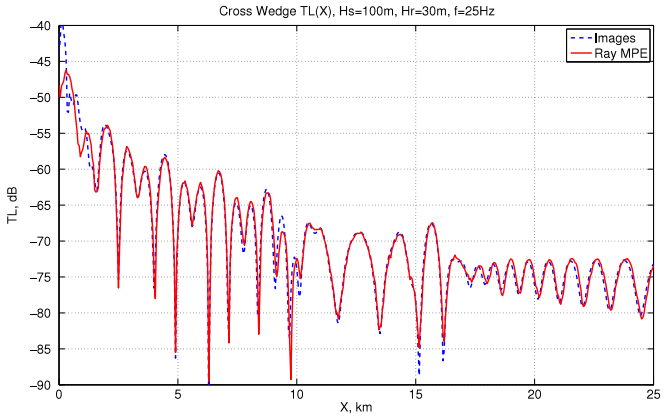

Fig. 2. The transmission loss for the ASA wedge, the source depth is 100 m. The receiver depth is 30 m, 3 modes, attenuation is 0.5 dB/λ. Propagation across the slope.

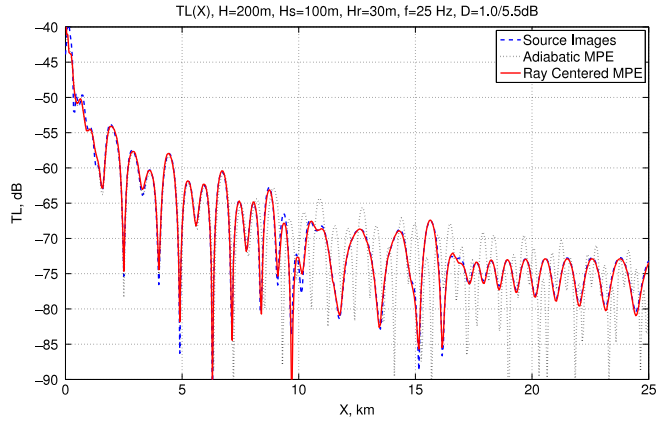

Fig. 3. The transmission loss for the ASA wedge, 7 modes, attenuation is 0.5 dB/λ. Propagation across the slope.

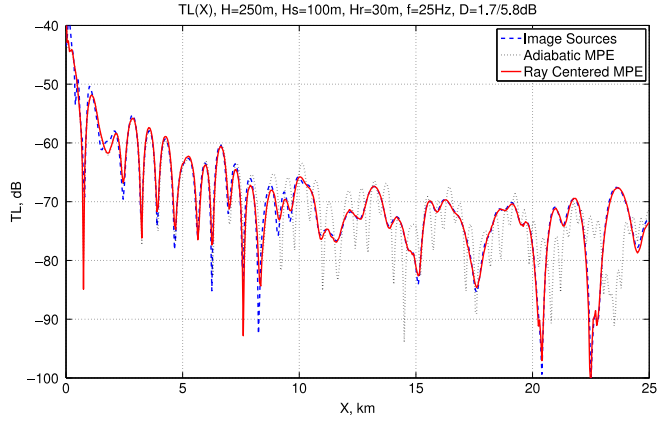

Fig. 4. The transmission loss for the ASA wedge, 7 modes, attenuation is 0.5 dB/λ. Propagation across the slope. The depth of watery layer is 250 m.

use more than 3 modes. For example, in the case of 7 modes (see Fig. 3), the field in the vicinity of the source is represented correctly, and the root mean square difference reduces to 1 dB. In both cases the bottom depth at the places of the source and the receivers was 200 m. In Fig. 3 the same results are presented for the case of the bottom depth 250 m and 7 propagating modes. Here the root mean square difference between curves is about 1.7 dB, and one can see pretty good coincidence of the curves from distance 10 km. Calculations by the adiabatic MPE [13] provide significantly worst accuracy.

Please cite this article in press as: M.Yu. Trofimov, et al., Mode Gaussian beam tracing, Computer Physics Communications (2016), http://dx.doi.org/10.1016/j.cpc.2016.06.002

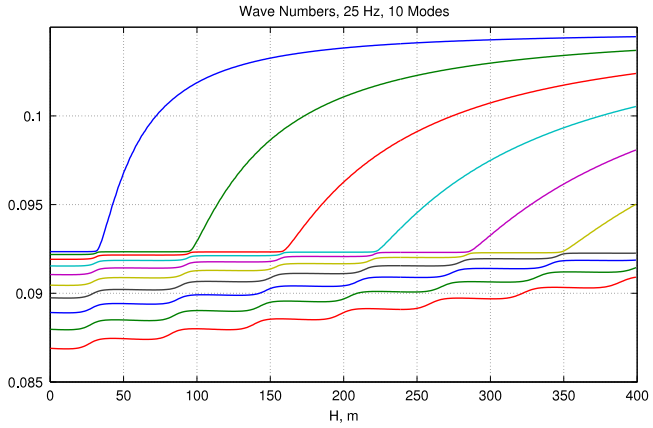

Fig. 5. The first 10 wavenumbers in dependence from the bottom depth of the ASA wedge at some point in X–Y plane.

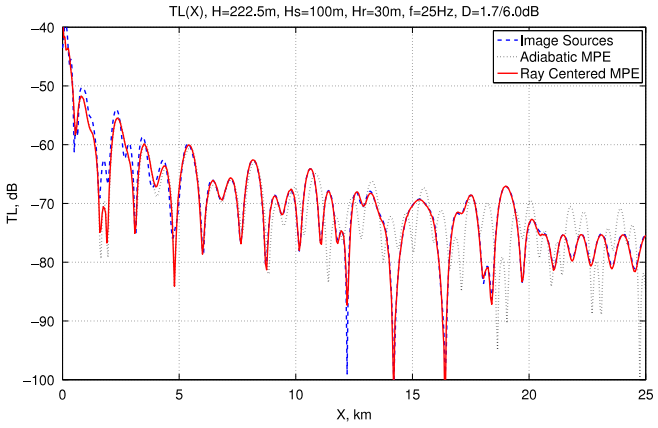

Fig. 7. The transmission loss for the ASA wedge, 7 modes, attenuation is 0.5 dB/λ. Propagation across the slope. The depth of watery layer is 222.5 m (resonant).

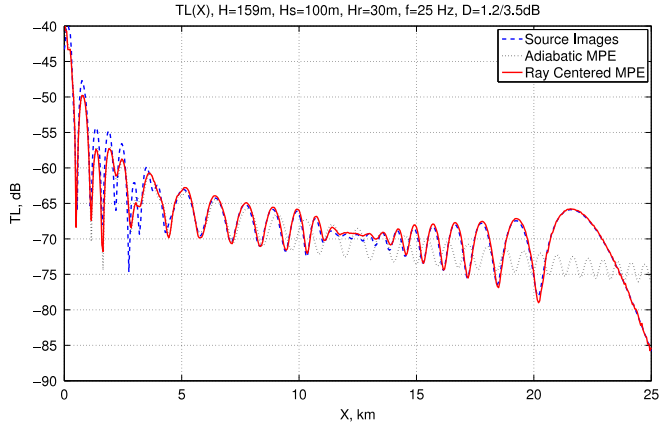

Fig. 6. The transmission loss for the ASA wedge. Propagation across the slope. The depth of watery layer is 159 m (resonant).

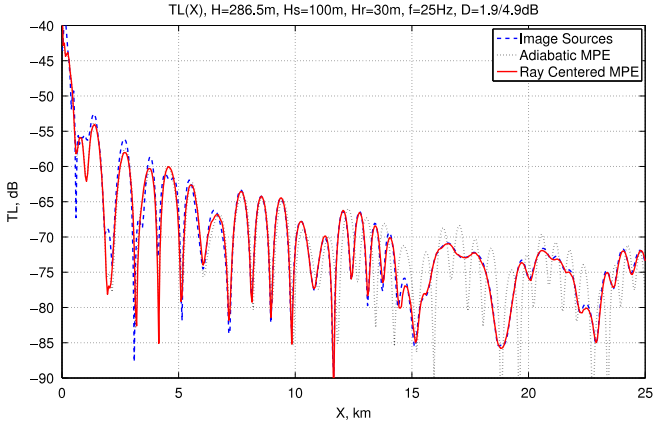

Fig. 8. The transmission loss for the ASA wedge. Propagation across the slope. The depth of watery layer is 286.5 m (resonant).

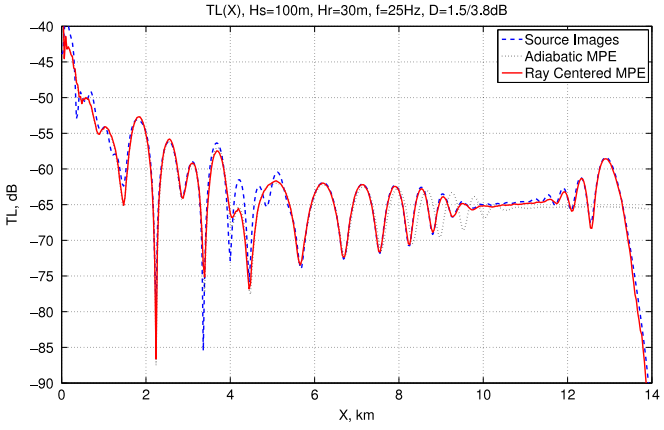

Fig. 9. The transmission loss for the ASA wedge, the source depth is 100 m. The receiver depth is 30 m, 7 modes, attenuation is 0.5 dB/λ. The track has an angle 12° to the cross-wedge direction.

Calculations by mode parabolic equations naturally split into two stages. In the first stage we calculate eigen numbers and functions in the considered area of the sound propagation, and determine the coefficients of the equations. In the second stage we solve the equations by some or other method and obtain the transmission losses in the places of the receivers. In our case the area has rectangular form 25 × 8 km. Due to uniformity of the problem on X variable it is sufficient to calculate the eigen numbers and functions only along the Y variable. We choose grid step on Y variable of 12.5 m to provide good accuracy. Angle step for the ray pattern calculations was 0.5°.

The calculation time for the 7-mode problem was about 81 s on the one core of the Intel® Core™2 Duo Processor E8400, 3.00 GHz. For the 3-mode problem the time of calculations was about 32 s.

In the second series of experiments (see Figs. 6–8), we also investigate the cross-slope sound propagation for the standard ASA wedge benchmark up to distance 25 km, but for the resonant bottom depth (see Fig. 5) in the sense of work [14]. In Fig. 6 the bottom depth is 159 m, which corresponds to the transformation of the 3rd mode. In Figs. 7 and 8 the bottom depths are 222.5 and 286.5 m, at which 4th and 5th modes transform respectively. The size of the area and the other parameters are the same as in the previous cases. The root mean square difference between curves is from 1.2 to 1.9 dB, so we can state, that the accuracy of calculations for the resonant depth is comparable with the one for the non-resonant bottom depth.

The third series of experiments (see Figs. 9–14) is devoted to the sound propagation with a small angle to the cross-slope direction for bottom depth 200 m at the source place. In our case the angles are ±12° for Figs. 9 and 10, ±18° for Figs. 11 and 12, ±24° for Figs. 13 and 14. One can see, that if for the angles ±12° the accuracy of the ray MPE is sufficiently good, then for the angles ±24° it becomes not so good. For the angles ±18° the accuracy has transitional behavior. This effect probably related with the necessity to take into account the mode interaction.

Please cite this article in press as: M.Yu. Trofimov, et al., Mode Gaussian beam tracing, Computer Physics Communications (2016), http://dx.doi.org/10.1016/j.cpc.2016.06.002

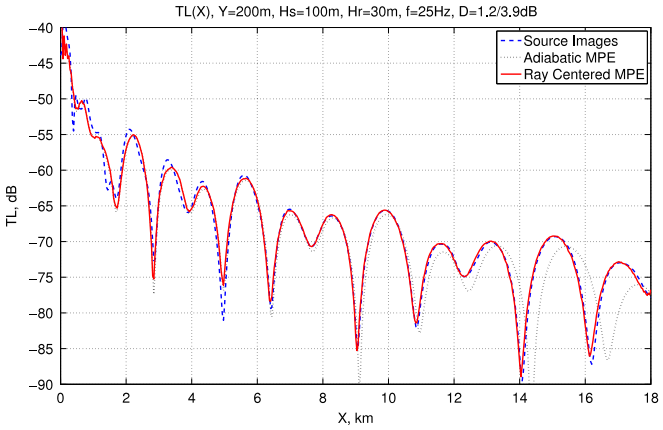

Fig. 10. The transmission loss for the ASA wedge, the source depth is 100 m. The receiver depth is 30 m, 7 modes, attenuation is 0.5 dB/λ. The track has an angle −12° to the cross-wedge direction.

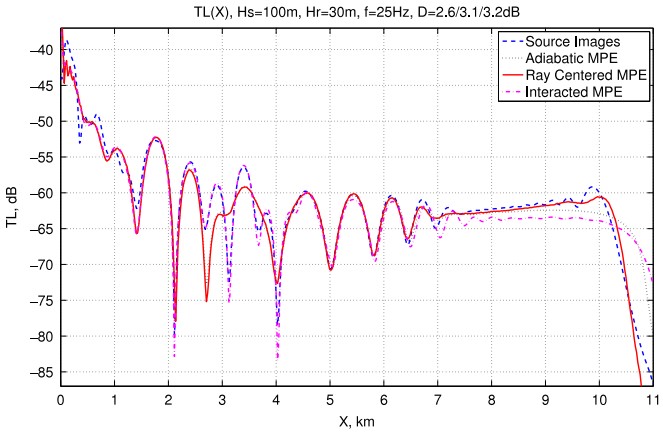

Fig. 11. The transmission loss for the ASA wedge, the source depth is 100 m. The receiver depth is 30 m, 7 modes, attenuation is 0.5 dB/λ. The track has an angle 18° to the cross-wedge direction.

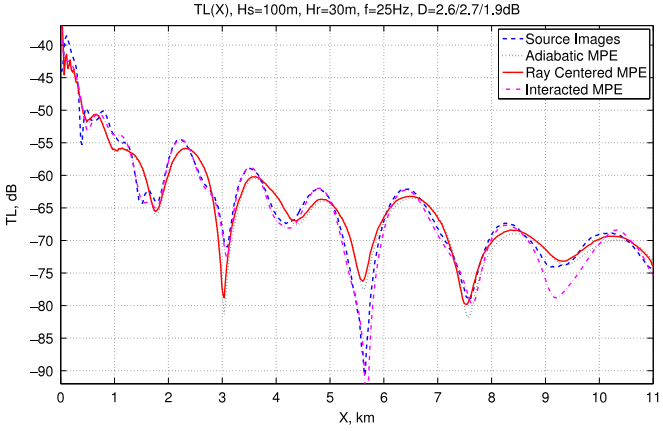

Fig. 12. The transmission loss for the ASA wedge, the source depth is 100 m. The receiver depth is 30 m, 7 modes, attenuation is 0.5 dB/λ. The track has an angle −18° to the cross-wedge direction.

6. Conclusions

The results of test calculations show that at small angles of the sound propagation track to the cross-wedge direction the acoustic field in the water is determined by the water modes only, without interaction between them, even in the case of the resonant depths. With the increase of the angle of the track to the cross-wedge direction the necessity to take into account the interaction between modes also increases, including the bottom modes.

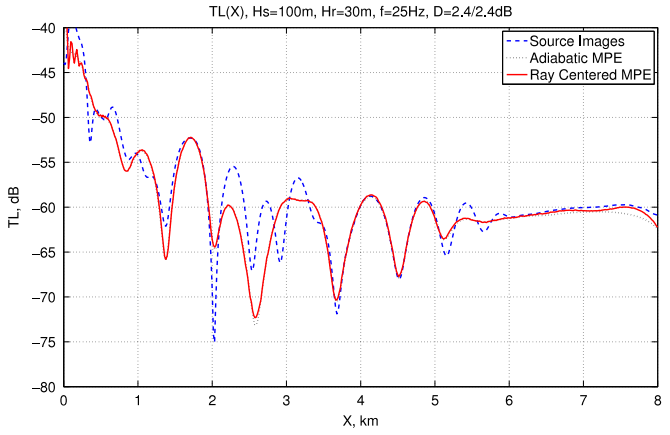

Fig. 13. The transmission loss for the ASA wedge, the source depth is 100 m. The receiver depth is 30 m, 7 modes, attenuation is 0.5 dB/λ. The track has an angle 24° to the cross-wedge direction.

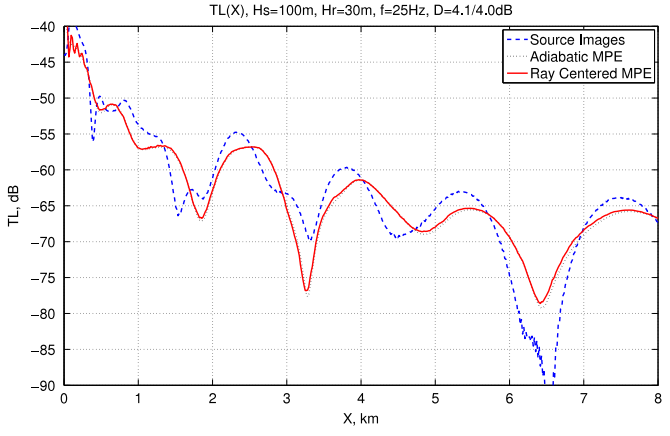

Fig. 14. The transmission loss for the ASA wedge, the source depth is 100 m. The receiver depth is 30 m, 7 modes, attenuation is 0.5 dB/λ. The track has an angle −24° to the cross-wedge direction.

As it is stated in the paper [8] concerning the speed of calculations by the modern 3D parabolic equation method: "In a MATLAB R2011a double precision programming environment, using one central-processing-unit core on an Intel® Xeon® X5492 Quad-core Processor, the Pade ADI method can complete one marching step in 54 s". It means that in the case of our ASA wedge cross-slope track with the length of 25 km the total number of marching steps is 2500. So the time of calculation should be around 37.5 h. Meanwhile, the time of calculations by the method developed in the current paper, with the use of the alike processor (mentioned above), consists only 32 s. Thus the developed method was proved to be very efficient in calculations of the acoustic fields. At present time we develop the method also based on the ray mode parabolic equations, but including the mode interaction. We hope that this method will be applicable to the case of an arbitrary environment.

Acknowledgment

The authors are grateful for the support of Exxon Neftegas Limited company (contract number A2294237DY0900).

References

[1] V. Červený, M.M. Popov, I. Pšenčík, Geophys. J. R. Astron. Soc. 70 (1982) 109–128.
[2] M.B. Porter, H.P. Bucker, J. Acoust. Soc. Am. 82 (4) (1987) 1349–1359.

[3] A.P. Kachalov, M.M. Popov, Sov. Phys. Docl. 26 (6) (1981) 604–606.
[4] V.M. Babich, M.M. Popov, Acoust. Phys. 27 (6) (1982) 459–462.
[5] M.M. Popov, Wave Motion 4 (1982) 85–97.
[6] V.E. Grikurov, M.M. Popov, Wave Motion 5 (1983) 225–233.
[7] R. Burridge, H. Weinberg, in: J.R. Keller, I.S. Papadakis (Eds.), Wave Propagation and Underwater Acoustics, in: Lecture Notes in Physics, vol. 70, Springer-Verlag, New-York, 1977.
[8] Y.T. Lin, J.M. Collis, T.F. Duda, J. Acoust. Soc. Am. 132 (5) (2012) EL364–EL370.
[9] F. Sturm, J. Acoust. Soc. Am. 117 (3) (2005) 1058–1079.
[10] A.H. Nayfeh, Perturbation Methods, John Wiley and Sons, New York, London, Sydney, Toronto, 1973.
[11] V.M. Babich, V.S. Buldyrev, Short-wavelength Diffraction Theory, Asymptotic Methods, Springer-Verlag, Berlin, Heidelberg, New York et al., 1991.
[12] G.B. Deane, M.J. Buckingham, J. Acoust. Soc. Am. 93 (1993) 1319–1328.
[13] M.Y. Trofimov, Acoust. Phys. 45 (1999) 575–580.
[14] M.Y. Trofimov, S.B. Kozitskiy, A.D. Zakharenko, Wave Motion 58 (2015) 42–52.

Please cite this article in press as: M.Yu. Trofimov, et al., Mode Gaussian beam tracing, Computer Physics Communications (2016), http://dx.doi.org/10.1016/j.cpc.2016.06.002